

# Mid-infrared PL relations for Globular Cluster RR Lyrae

A. K. Dambis<sup>\*</sup>, A. S. Rastorguev and M. V. Zabolotskikh

*Sternberg Astronomical Institute, Lomonosov Moscow State University, Universitetskii pr. 13, Moscow, 119992 Russia*

Accepted 2014 January 31. Received 2014 January 21; in original form 2013 October 14

## ABSTRACT

The period - metallicity - WISE W1- and W2-band luminosity relations are derived for RR Lyrae stars based on WISE epoch photometry for 360 and 275 stars in 15 and 9 Galactic globular clusters, respectively. Our final relations have the form  $\langle M_{W1} \rangle = \gamma_{W1} - (2.381 \pm 0.097) \log P_F + (0.096 \pm 0.021) [\text{Fe}/\text{H}]$  and  $\langle M_{W2} \rangle = \gamma_{W2} - (2.269 \pm 0.127) \log P_F + (0.108 \pm 0.021) [\text{Fe}/\text{H}]$ , where  $[\text{Fe}/\text{H}]$  values are on the scale of Carretta et al. (2009). We obtained two appreciably discrepant estimates for the zero points  $\gamma_{W1}$  and  $\gamma_{W2}$  of both relations: one based on a statistical-parallax analysis –  $\gamma_{W1} = -0.829 \pm 0.093$  and  $\gamma_{W2} = -0.776 \pm 0.093$  and another, significantly brighter one, based on HST FGS trigonometric parallaxes –  $\gamma_{W1, HST} = -1.150 \pm 0.077$  and  $\gamma_{W2, HST} = -1.105 \pm 0.077$ . The period-metallicity-luminosity relations in the two bands yield highly consistent distance moduli for the calibrator clusters and the distance moduli computed using the W1- and W2-band relations with the HST zero points agree well with those computed by Sollima et al. (2006) based on their derived period-metallicity-K-band luminosity relation whose zero point is tied to the HST trigonometric parallax of RR Lyrae itself ( $\Delta DM_0 = 0.04$  and  $0.06$ , respectively, with a scatter of only  $0.06$ ).

**Key words:** stars: variables: RR Lyrae; stars: distances; Galaxy: globular clusters; infrared: stars

## 1 INTRODUCTION

RR Lyrae variables are known to obey rather tight period-metallicity-luminosity relations of the form

$$\langle M_X \rangle = \alpha_X \cdot \log P_F + \beta_X \cdot [\text{Fe}/\text{H}] + \gamma_X, \quad (1)$$

where  $\langle M_X \rangle$  is the intensity-mean absolute magnitude in the photometric band X and  $P_F$  is the fundamental-mode period (equal to the variability period  $P$  for RRab type variables, which pulsate in the fundamental mode and  $\log P_F = \log P + 0.127$  or  $P_F = P/0.746$  – for RRc type variables, which pulsate in the first overtone) in various photometric bands X (Catelan et al. 2004). (The above first-overtone to fundamental period ratio dates back to theoretical estimates by Iben (1974) and is commonly used by most of the authors to fundamentalise the periods of RRc type variables – see, e.g., Frolov & Samus (1998); Sollima et al. (2006); Feast et al. (2008). Earlier model-based estimates yield a period conversion factor corresponding to  $\log P_F = \log P + 0.130$  (van Albada & Baker 1973). More recent stellar models corroborate these results and, as Castellani et al. (1997) point out, show that the adopted procedure yields fundamentalised periods with an uncertainty no larger than  $\delta \log P_F = \pm 0.005$  (Bono et al. 1997; Marconi et al. 2003). Further support for the small uncertainty is provided by the

observed period ratios of double-mode RR Lyrae type stars (RRd) – as is evident from the Petersen diagram for Galactic and LMC RRd type stars shown in Fig. 2 in Poleski (2013), the period ratios in all these objects are constrained to the narrow interval from 0.742 to 0.748 corresponding to the interval of logarithmic corrections from  $+0.126$  to  $+0.130$ ). It is these relations that make RR Lyraes very popular standard candles used extensively to estimate distances to stellar systems harbouring old populations. Recently, mid-infrared light curves have been acquired for several thousand RR Lyraes as a result of spaceborne WISE all-sky photometric survey (Wright et al. 2010), and hence establishing the period-metallicity-luminosity relations for these stars at least in some of the WISE bands has become a task of prime importance. The progress so far achieved in this direction includes (1) a study by Klein et al. (2011), who found  $\alpha_{W1} = (1.681 \pm 0.147)$  with no evidence for metallicity term  $\beta_{W1}$  by computing posterior distances of 76 well observed RR Lyrae based on the optically constructed prior distances; (2) a conclusion by Dambis et al. (2013) that the period and metallicity slopes of the W1-band PML relation are practically identical to those of the  $K_s$ -band PML relation ( $\alpha_K = \alpha_{W1} = -2.33$  and  $\beta_K = \beta_{W1} = +0.088$ ) based on the small scatter of the estimated  $\langle K_s \rangle - \langle W1 \rangle$  intrinsic colour indices of Galactic field RR Lyraes with known metallicities, and (3) the study of Madore et al. (2013), who derived WISE W1, W2, and W3-band RR Lyrae PL rela-

<sup>\*</sup> E-mail: mirage@sai.msu.ru

tions based on the trigonometric parallaxes of four Galactic field RR Lyraes. The problem with the results of Klein et al. (2011) is that these authors do not fundamentalise the periods of c-type RR Lyraes, which is evidently a bad idea given that RRc type stars form a well-defined  $\Delta \log(P) = -0.127$  period-shifted branch of the PL relation in the  $K$  band ( $\lambda_{eff} \sim 2.2 \mu m$ ) and there are no reasons for RR Lyrae variables to behave differently in the W1 band ( $\lambda_{eff} \sim 3.4 \mu m$ ). The conclusion of Dambis et al. (2013) might not be entirely correct, because the small scatter of computed ( $\langle K_s \rangle - \langle W1 \rangle_0$ ) intrinsic colour indices may be a result of the star-to-star variations of the period and metallicity terms cancelling each other because of the appreciable correlation between  $\log P_F$  and  $[Fe/H]$ . Finally, the slopes of the W1, W2, and W3-band PL relations estimated by Madore et al. (2013) have large errors because of the very small number of stars involved (four). It therefore makes sense to try to estimate the period slopes of the RR Lyrae PML relation in some of the WISE bands in a way that would eliminate the effect of metallicity term.

In this study we follow the footsteps of Sollima et al. (2006) and use photometric data for RR Lyrae variables in globular clusters to derive the period slopes ( $\alpha$ ) for the RR Lyrae PML relation in the WISE W1 and W2 bands, because, as the above authors point out, "The advantage of using GCs in constraining the coefficients  $\alpha$ ,  $\beta$  and  $\gamma$  lies in the fact that all the stars in a given cluster are at the same distance, and can be considered to share the same metal content and be subject to the same extinction effect." We then estimate the corresponding metallicity slopes ( $\beta$ ) of these relations based on photometric data for field RR Lyrae type variables with known  $[Fe/H]$ , and, finally, infer the zero points ( $\gamma$ ) of the corresponding relations based on (1) results of statistical-parallax-analysis by Dambis et al. (2013) and (2) HST FSG trigonometric parallaxes.

## 2 THE DATA

Last year, the WISE All-Sky Data Release (Cutri et al. 2012) was made public, mapping the entire sky in four mid-infrared bands W1, W2, W3, and W4 with the effective wavelengths of 3.368, 4.618, 12.082 and 22.194  $\mu m$ , respectively (Wright et al. 2010). We cross-correlated the WISE single-exposure database with the Catalogue of Galactic globular-cluster variables by Clement et al. (2001), the Catalogue of Accurate Equatorial Coordinates for Variable Stars in Globular Clusters by Samus et al. (2009), and the catalogue of Sawyer Hogg (1973) (for  $\omega$  Cen, NGC6723, and NGC6934) to compute (via Fourier fits) the intensity-mean average W1- and W2- band magnitudes,  $\langle W1 \rangle$  and  $\langle W2 \rangle$ , for a total of 357 and 272 RR Lyrae type variables in 15 and 9 Galactic globular clusters, respectively. Figures 1 and 2 show examples of W1- and W2-band light curves of different quality. As is evident from these samples, the phase coverage is more or less satisfactory in most of the cases, although the quality of the light curves differs greatly. The order of the Fourier fit naturally depends on the light-curve quality with only the constant term is left for the poorest curves.

The list of 360 globular-cluster RR Lyrae type stars used in this study is presented in Table 1 (its full version

will be available from the CDS). The columns of this table provide the following information: (1) NGC designation of the cluster; (2) other commonly used name of the cluster; (3) name of the variable; (4) variability period in days; (5) W1-band intensity-mean magnitude with (6) its standard error; (7) W2-band intensity-mean magnitude with (8) its standard error; (9) variability type (RR0, RR1, and RR2 indicate type ab, c, and d variables, respectively, and RR9 indicates variables with unknown subtypes), and (10) a flag indicating whether the particular variable was used in the final PL relation fit (1 - used and 0 - rejected).

A potential source of error is the Blazhko effect – long-period variations of the form and amplitude of the light curve – exhibited by some RR Lyraes. There are known Blazhko stars in five clusters of our list: M3, M5, M15, NGC3201, and NGC5466. The Blazhko effect should not introduce appreciable errors in the computed intensity-mean magnitudes for stars in M15 and NGC3201 because the time span covered by WISE observations in these clusters ( $\sim 1.1$  and 3.9 days, respectively) is short compared to typical Blazhko periods, which are on the order of several dozen days. Each of our RR Lyr star in M3 has 14 WISE measurements including 12 observations concentrated within a  $\sim 1.4$ -day interval (MJD 55375.074090–55376.463216) and two observations near MJD 55203.412309. However, we found that the inclusion/exclusion of the two "outlying" observations has no appreciable effect on the computed intensity-mean averages in either W1 or W2 with the differences not exceeding  $0.009^m$  and  $0.046^m$ , respectively (the standard errors of the computed intensity means are greater than  $0.012^m$  and  $0.042^m$  in W1 and W2, respectively, for all the stars concerned). WISE observations of RR Lyraes in M5 were made within two epoch intervals (MJD 55411.716751 – 55412.708967 and 55231.073846 – 55234.315989) including 12 and 22 measurements, respectively. The light curves for the two intervals differ appreciably, and the computed intensity means differ by less than  $0.067^m$  and  $0.130^m$  in W1 and W2, respectively. The intensity means based on all observations and computed ignoring the variation of the light-curve shape and amplitude differ from the intensity-means based on each of the "quasi-simultaneous" light curves by less than  $0.041^m$  and  $0.075^m$  in W1 and W2, respectively. However, the averages of the intensity means computed separately for the two epoch intervals practically coincide with the corresponding intensity means computed based on all available observations ignoring the Blazhko variations: the differences do not exceed  $0.015^m$  and  $0.010^m$  in W1 and W2, respectively. In NGC5466 each star has only two "outlying" measurements (about MJD 55203.080975), while the bulk of observations (15 measurements) are concentrated within a  $\sim 1.1$ -day long interval (MJD 55380.630970 – 55381.755488). The inclusion/exclusion of the two "rogue" measurements has negligible effect on the final intensity means with the differences not exceeding  $0.009^m$  and  $0.050^m$  in W1 and W2, respectively (the standard errors are greater than  $0.037^m$  and  $0.074^m$  in W1 and W2, respectively, for all the stars concerned). Given the smallness of the Blazhko-variation due effect on the inferred intensity means and the small fraction of Blazhko stars in our sample (15 out of 73-74 stars in M3, 3 out of 36 stars in M5, 6 out of 28 stars in M15, 1 out of 58 stars in NGC3201, and 2 out of 9 stars in NGC5466 with no Blazhko stars in other clusters) hereafter we adopt

**Table 1.** The data for RR Lyrae in the calibrator GCs. This is a sample of the full version, which is available in the online version of the article (see Supporting Information).

Cluster name	Alternative cluster name	Variable name	Period, days	$\langle W1 \rangle$	$\sigma \langle W1 \rangle$	$\langle W2 \rangle$	$\sigma \langle W2 \rangle$	Type	Use/Reject
NGC3201		V003	0.5994	12.3083	0.0201	12.3628	0.0239	RR0	0
NGC3201		V004	0.6300	12.6777	0.0145	12.6880	0.0235	RR0	1
NGC3201		V006	0.5253	12.8124	0.0286	12.8956	0.0269	RR0	1
NGC3201		V007	0.6303	12.6029	0.0090	12.6673	0.0230	RR0	1
NGC3201		V008	0.6287	12.5628	0.0333	12.5852	0.0581	RR0	1
NGC3201		V009	0.5255	12.6367	0.0150	12.6491	0.0253	RR0	1
NGC3201		V010	0.5352	12.7077	0.0203	12.6578	0.0242	RR0	1
NGC3201		V011	0.2990	11.4651	0.0118	11.5245	0.0304	RR1	0
NGC3201		V012	0.4956	12.7398	0.0199	12.8645	0.0361	RR0	1
NGC3201		V013	0.5752	12.4619	0.0219	12.4421	0.0234	RR0	0

**Table 2.** The sample of calibrator GCs. Metallicities are in the CG scale.

Name	[Fe/H]	E(B-V)	Number of RR Lyr (W1)	(W2)
M3	-1.50	0.01	74	73
M4	-1.16	0.35	31	31
M5	-1.29	0.03	36	36
M15	-2.37	0.10	28	
M53	-2.10	0.02	22	
M55	-1.94	0.08	6	6
M92	-2.31	0.02	7	7
M107	-1.02	0.33	9	9
NGC 3201	-1.59	0.24	58	58
NGC 5053	-2.27	0.01	8	
NGC 5466	-1.98	0.00	9	
NGC 6362	-0.99	0.09	17	17
NGC 6723	-1.10	0.05	9	
NGC 6934	-1.47	0.10	8	
$\omega$ Cen	-1.75*	0.12	38	38

\* Because of the well known metallicity spread among RR Lyrae stars in this cluster (Sollima et al. 2006 and reference therein), we took into account only the metal-poor ( $[Fe/H] < -1.4$ )

the intensity mean W1- and W2-band magnitudes computed based on all available WISE observations for all stars ignoring eventual light-curve variations. Figure 3 shows several examples of Blazhko star light curves in three clusters.

Table 2 lists the data for our calibrator GCs including the number of RR Lyrae found with adopted WISE W1- and W2-band light curves as well as the metallicity in the scale of Carretta et al. (2009) and the reddening E(B-V), both adopted from the updated version of the globular-cluster catalogue by Harris (1996) (Harris 2010).

### 3 CALIBRATION OF THE PML RELATION

So far, three studies involved the estimation of the parameters of the period-metallicity-luminosity relation in the form of eq. (1) for WISE mid-infrared photometric bands, all of them based on field stars. We summarise the correspond-

**Table 3.** Published determinations of the parameters of the RR Lyrae period-metallicity-luminosity relations in WISE photometric bands.

Ref.	Filter	$\alpha$	$\beta$	$\gamma$
K11	W1	-1.681		+0.083
K11	W2	-1.715		+0.092
K11	W3	-1.688		+0.013
D13	W1	-2.33	0.088	-0.825
M13	W1	-2.44		-1.26
M13	W2	-2.55		-1.29
M13	W3	-2.58		-1.32

References: K11: Klein et al. (2011); D13: Dambis et al. (2013); M13: Madore et al. (2013).

ing results in Table 3. Given eq. (1), the apparent X-band magnitude of a particular star is equal to

$$\langle X \rangle = \alpha_X \log P_F + \beta_X [Fe/H] + \gamma_X + (m - M)_0 + A_X, \quad (2)$$

where  $\langle X \rangle$  is the intensity-mean X-band magnitude;  $(m - M)_0$ , the true distance modulus, and  $A_X$ , the total extinction in the X band.

We now proceed to determine the three parameters (coefficients)  $\alpha_X$ ,  $\beta_X$ , and  $\gamma_X$  of eq. (1) for the two shortest-wavelengths WISE passbands X=W1 and X=W2 from observational data.

#### 3.1 The period slopes ( $\alpha_X$ )

All stars in a particular cluster can be considered to be at the same distance (which is much greater than the size of the cluster and hence the line-of-sight extent of the system can be neglected) and (in most cases) to have the same metallicity and the same amount of interstellar extinction (anyway, intracluster extinction variations in all WISE photometric bands are at least about a factor of 17 smaller than the corresponding variations in the V-band extinction (Yuan et al. 2013) and therefore negligible). Equation (2) for stars of a given cluster then acquires the form

$$\langle X \rangle - \alpha_X (\log P_F + 0.25) = C_X \quad (3)$$

where  $C_X = \beta_X [Fe/H] + \gamma_X + (m - M)_0 + A_X - 0.25\alpha_X$  can be considered to be a constant. Hereafter we add the +0.25 term to  $\log P_F$  in order to centre the solution at  $\log P_F = -0.25$ ,

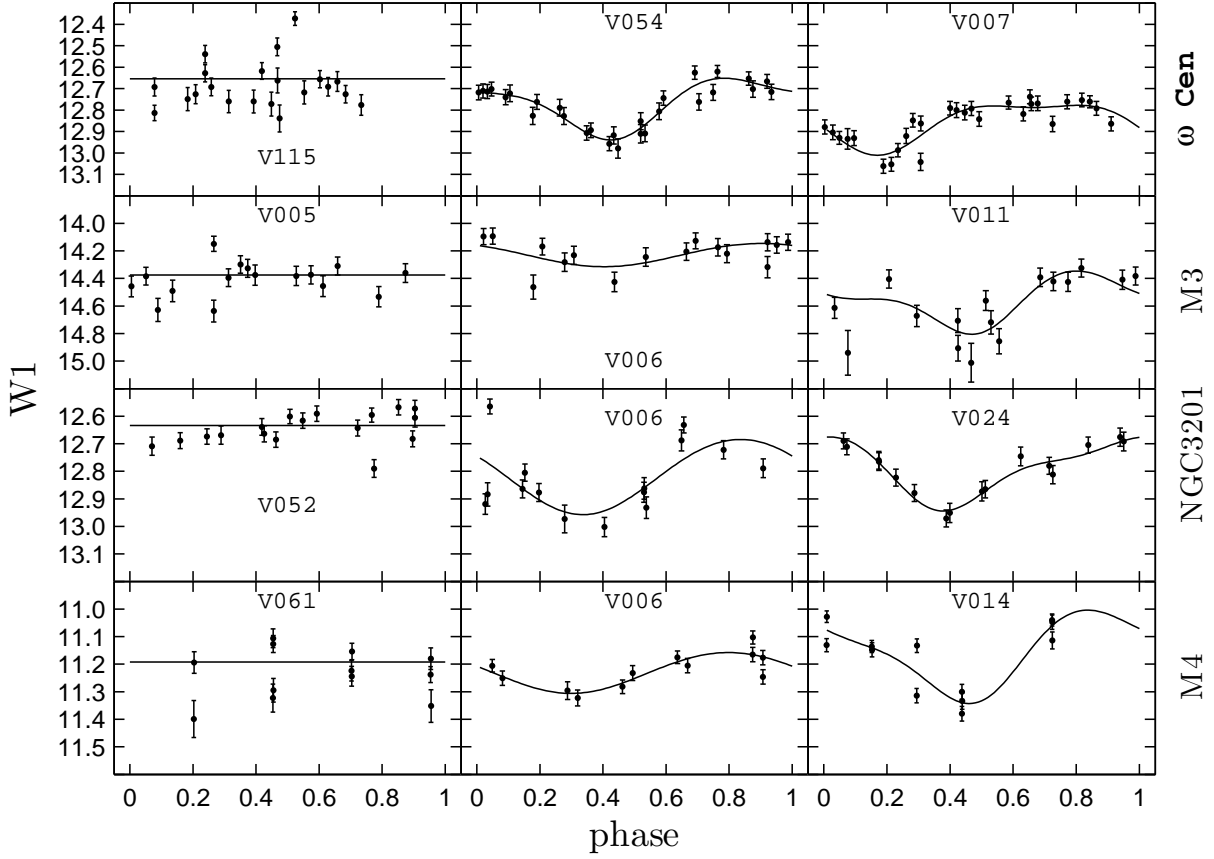


**Figure 1.** Examples of RR Lyrae type star W1-band light curves of various quality in four globular clusters.

which is close to the average value of this parameter, so as to make the  $C_X$  constant more representative of the cluster distance modulus and minimise the effect of differences in the inferred  $\alpha_X$  values between different clusters. We use the following heuristic procedure to estimate the constant  $C_X$  for some assumed slope  $\alpha_X$ . We compute the left-hand side of eq. (3)  $c_{\alpha,i} = \langle X \rangle - \alpha_X (\log P_{F,i} + 0.25)$  for each star. We then sort the  $C_{\alpha,i}$  values in the ascending order and seek the subset  $\mu = \{j, j+1 \dots j+N_1-1\}$  containing  $N_1 = N \times q$  values with  $q=0.68$  (where  $N$  is the total number of RR Lyraes in the given cluster for which we determined the corresponding X-band intensity mean magnitudes) having the smallest dispersion of computed  $C_\alpha$  values,  $\sigma C_{\alpha,\mu}$  (we adopt  $q=0.8$  for NGC5053 and M92 and  $q=1.0$  for NGC6934). We then try  $\alpha$  values from -1.0 to -5.0 in increments of 0.01 to find the one yielding the smallest  $\sigma C_{\alpha,\mu}$ . If the modal "core" distribution (i.e., the part of the distribution corresponding to stars whose data points outline the purported linear  $\log P_F - \langle X \rangle$  relation) of  $C_i$  values were normal, our subset would roughly consist at least of all stars with  $C_j$  between the  $\langle C \rangle - \sigma C$  and  $\langle C \rangle + \sigma C$ , where  $\langle C \rangle$  and  $\sigma C$  are the mean and dispersion of  $C$  values for the subset of stars defining the linear  $\log P_F - \langle X \rangle$  relation, respectively. The mean  $C$  value averaged over the subset stars,  $\langle C_\mu \rangle$ , should then be close to the mean  $\langle C \rangle$ , and the (truncated) dis-

persion  $\sigma C_\mu$  should be roughly equal to  $\sigma C_{subset} = 0.54\sigma C$  and hence  $3\sigma C = 5.56\sigma C_{subset}$ . We therefore determine the final estimate of  $C$  and  $\alpha_X$  by least-squares solving the equation set

$$\alpha_X (\log P_F + 0.25) + C = \langle X \rangle, \quad (4)$$

(it is just a rewritten form of eq. (3)) for stars with  $C_\mu$  values in the interval  $\langle C_\mu \rangle - 5.56\sigma C_\mu \leq C_\mu \leq \langle C_\mu \rangle + 5.56\sigma C_\mu$ . The resulting solutions (i.e., the  $\alpha_X$  and  $C_X$  values, their standard errors and the standard error of  $\langle X \rangle$ , where  $X=W1$  or  $W2$ ) for all globular clusters, where such solutions could be reasonably derived, are listed in Table 4. Like Sollima et al. (2006), we plot the scaled W1 and W2 magnitudes ( $W1 - C_{W1}$  and  $W2 - C_{W2}$ ) for our calibrating clusters as a function of fundamentalised periods in Figs. 4 and 5, respectively.

Figures 6 and 7 show the individual cluster slopes  $\alpha_{W1}$  and  $\alpha_{W2}$  as a function of metallicity. Linear least squares analysis yields the following results concerning the possible metallicity dependence of the slopes  $\alpha_{W1}$  and  $\alpha_{W2}$ :

$$\alpha_{W1} = -2.441 \pm 0.101 - (0.46 \pm 0.21)([Fe/H] + 1.5) \quad (5)$$

and

$$\alpha_{W2} = -2.311 \pm 0.127 - (0.23 \pm 0.31)([Fe/H] + 1.5). \quad (6)$$

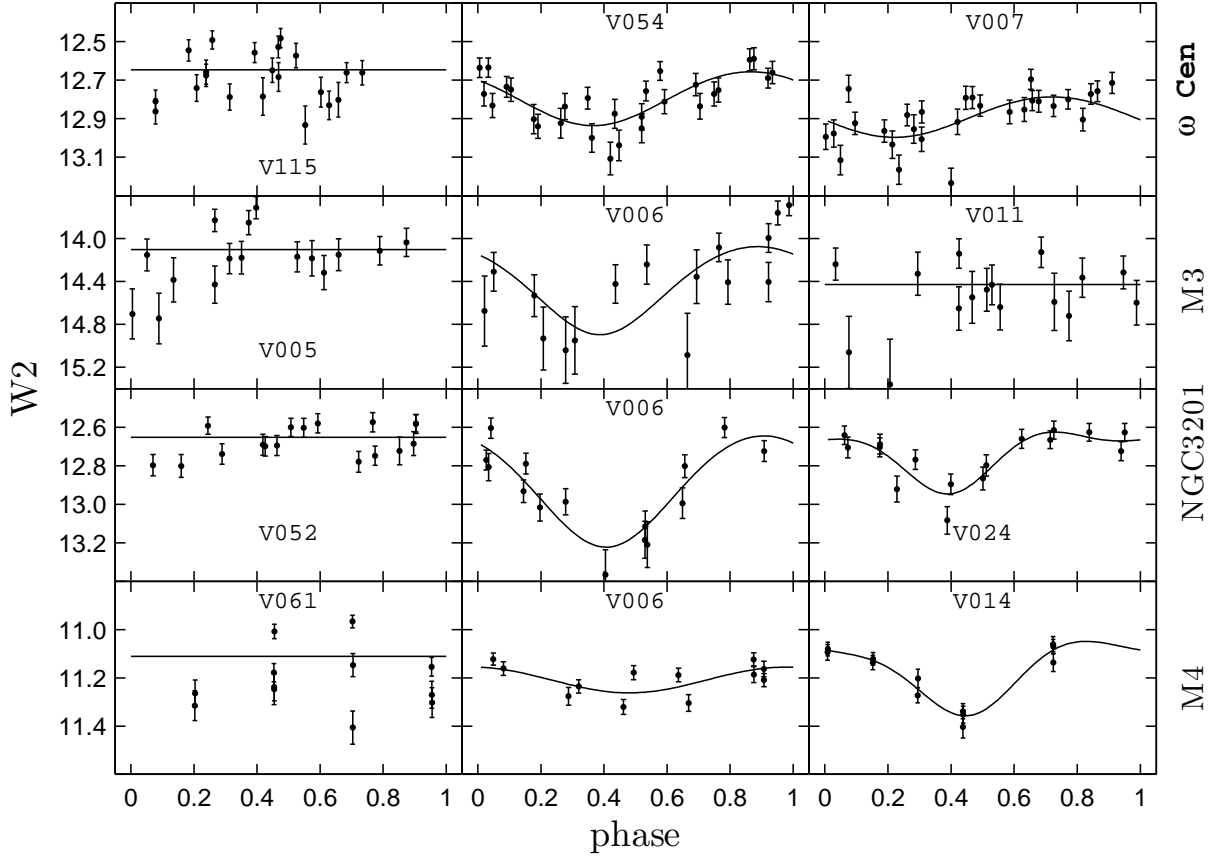


**Figure 2.** Examples of RR Lyrae type star W2-band light curves of various quality in four globular clusters.

**Table 4.** Parameters of the  $\langle W1 \rangle = \alpha_{W1} (\log P_F + 0.25) + C_{W1}$  and  $\langle W2 \rangle = \alpha_{W2} (\log P_F + 0.25) + C_{W2}$  fits for the globular clusters of our sample.

Name	$\alpha_{W1}$	$C_{W1}$	$\sigma \langle W1 \rangle$	$\alpha_{W2}$	$C_{W2}$	$\sigma \langle W2 \rangle$
M3	$-2.235 \pm 0.256$	$14.410 \pm 0.016$	0.124	$-1.642 \pm 0.332$	$14.383 \pm 0.021$	0.161
M4	$-2.694 \pm 0.213$	$10.818 \pm 0.020$	0.082	$-2.540 \pm 0.248$	$10.817 \pm 0.024$	0.096
M5	$-2.343 \pm 0.236$	$13.770 \pm 0.020$	0.098	$-2.225 \pm 0.321$	$13.824 \pm 0.027$	0.134
M15	$-2.013 \pm 0.445$	$14.382 \pm 0.036$	0.156			
M53	$-2.588 \pm 0.580$	$15.542 \pm 0.044$	0.193			
M55	$-1.817 \pm 0.207$	$13.004 \pm 0.013$	0.025	$-2.294 \pm 0.553$	$12.997 \pm 0.036$	0.068
M92	$-2.516 \pm 0.969$	$13.766 \pm 0.087$	0.138	$-2.379 \pm 0.665$	$13.795 \pm 0.060$	0.095
M107	$-2.158 \pm 0.319$	$13.214 \pm 0.035$	0.083	$-2.210 \pm 0.314$	$13.196 \pm 0.035$	0.082
NGC 3201	$-2.284 \pm 0.306$	$12.791 \pm 0.016$	0.106	$-2.112 \pm 0.343$	$12.797 \pm 0.018$	0.118
NGC 5053	$-2.071 \pm 0.495$	$15.512 \pm 0.038$	0.089			
NGC 5466	$-1.729 \pm 0.531$	$15.409 \pm 0.045$	0.103			
NGC 6362	$-3.167 \pm 0.384$	$13.742 \pm 0.051$	0.138	$-3.034 \pm 0.544$	$13.803 \pm 0.072$	0.195
NGC 6723	$-2.894 \pm 0.583$	$14.012 \pm 0.055$	0.105			
NGC 6934	$-2.990 \pm 0.898$	$15.459 \pm 0.047$	0.100			
$\omega$ Cen	$-2.158 \pm 0.197$	$13.115 \pm 0.018$	0.087	$-2.409 \pm 0.222$	$13.152 \pm 0.020$	0.098

The slope  $\alpha_{W2}$  appears to be independent of metallicity, whereas there seems to be hint of a dependence in the case of  $\alpha_{W1}$ . However, even in the latter case the slope differs from zero by less than  $2.2\sigma$  and we therefore derive the combined solutions for both photometric bands (see Figs. 8 and 9),

yielding the final slopes of  $\alpha_{W1} = -2.381 \pm 0.098$  and  $\alpha_{W2} = -2.269 \pm 0.127$ . Table 5 lists the resulting  $C_{W1}$  and  $C_{W2}$  values obtained in terms of these solutions (i.e., by forcing the same slope for all clusters).

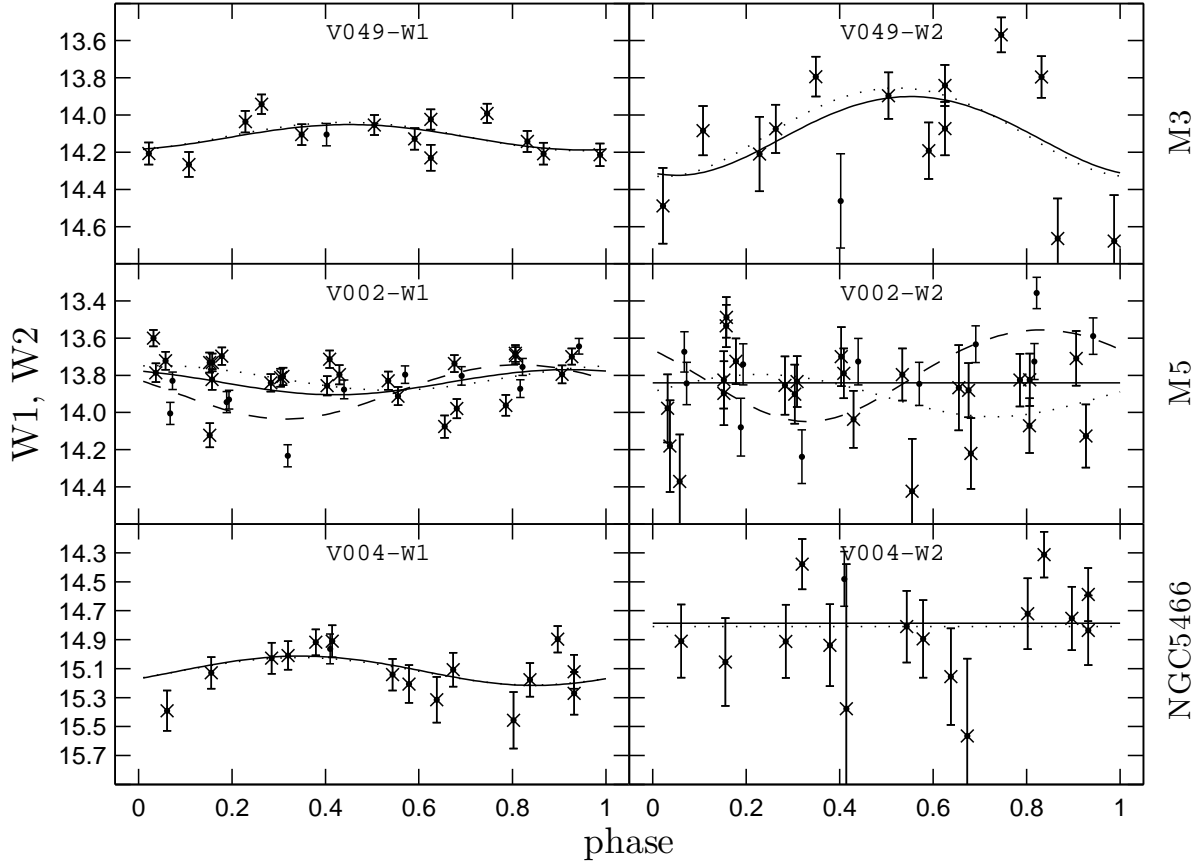


**Figure 3.** Examples of W1- (left) and W2-band (right) light curves of some Blazhko RR Lyrae variables in M3, M5, and NGC5466. The crosses and dots show the measurements corresponding to the "first" and "second" epoch intervals, respectively. The dotted and dashed curves show the light-curve fits based on the "first" and "second" epoch intervals, respectively, and the solid curves, the light-curve fits based on all available measurements.

**Table 5.** Parameters  $C_{W1}$  and  $C_{W2}$  of the combined  $\langle W1 \rangle = \alpha_{W1} (\log P_F + 0.25) + C_{W1}$  and  $\langle W2 \rangle = \alpha_{W2} (\log P_F + 0.25) + C_{W2}$  single-slope fits for the globular clusters of our sample ( $\alpha_{W1} = -2.381 \pm 0.098$  and  $\alpha_{W2} = -2.269 \pm 0.127$ ).

Name	$C_{W1}$	$C_{W2}$
M3	$14.407 \pm 0.015$	$14.369 \pm 0.027$
M4	$10.836 \pm 0.024$	$10.834 \pm 0.027$
M5	$13.768 \pm 0.022$	$13.822 \pm 0.025$
M15	$14.373 \pm 0.027$	
M53	$15.544 \pm 0.027$	
M55	$13.000 \pm 0.054$	$12.997 \pm 0.061$
M92	$13.766 \pm 0.061$	$13.792 \pm 0.069$
M107	$13.200 \pm 0.041$	$13.192 \pm 0.046$
NGC 3201	$12.789 \pm 0.017$	$12.794 \pm 0.020$
NGC 5053	$15.518 \pm 0.046$	
NGC 5466	$15.425 \pm 0.046$	
NGC 6362	$13.817 \pm 0.032$	$13.876 \pm 0.036$
NGC 6723	$14.035 \pm 0.050$	
NGC 6934	$15.466 \pm 0.050$	
$\omega$ Cen	$13.124 \pm 0.022$	$13.146 \pm 0.025$

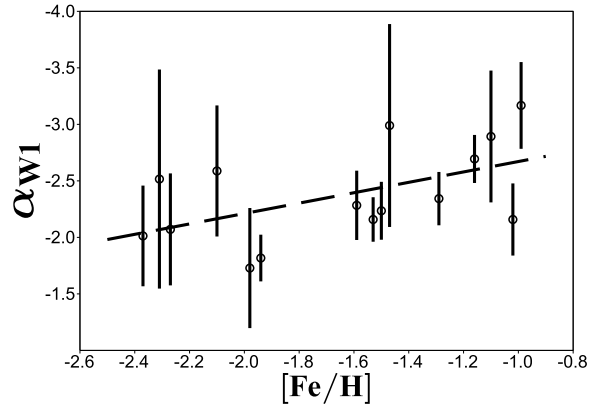


**Figure 6.** The parameter  $\alpha_{W1} = \delta M_{W1} / \delta \log P$  for RR Lyrae stars as a function of the cluster metallicity. The dashed line shows the relation defined by equation (5).

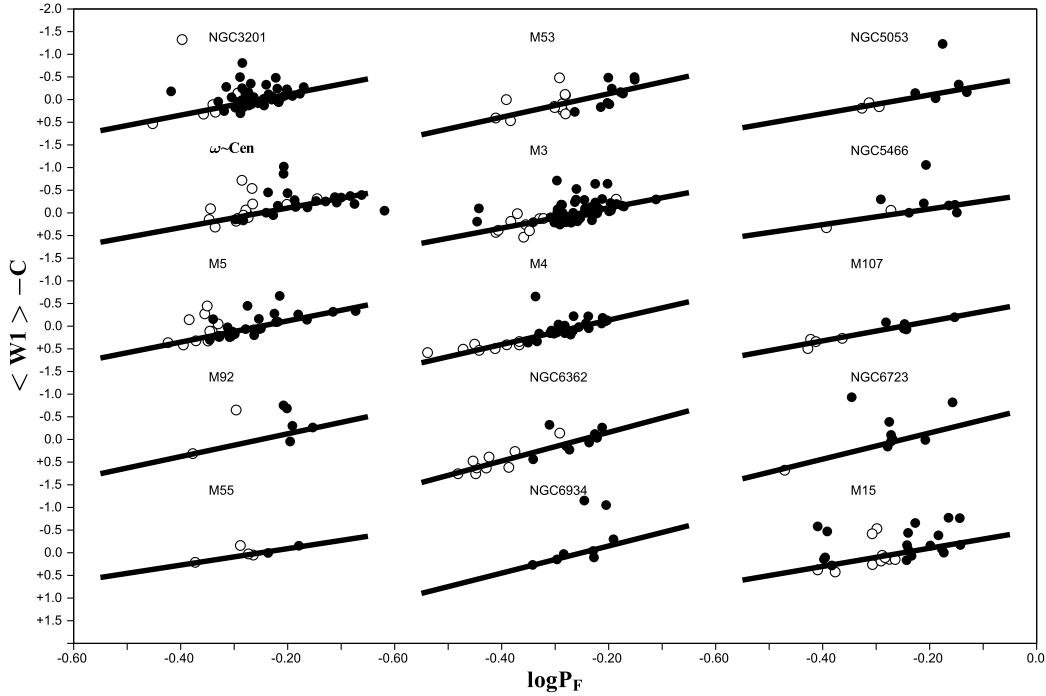


**Figure 4.** The  $PL_{W1}$  relation for the RR Lyrae in 15 calibrator globular clusters. The filled and open circles are the RRab and RRc type variables with fundamentalised periods, respectively. The W1 magnitudes are scaled to the same distance, extinction, and metallicity by subtracting the parameter  $C_{W1}$  for each cluster.

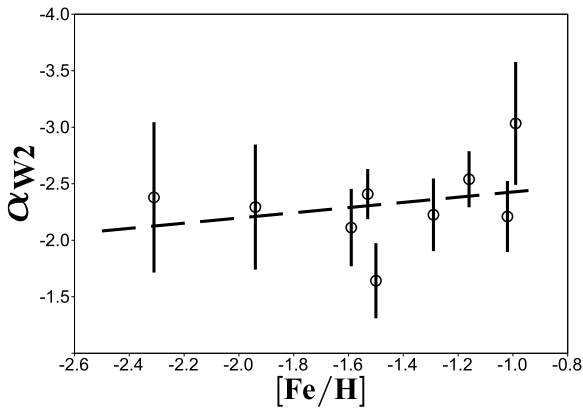


**Figure 7.** The parameter  $\alpha_{W2} = \delta M_{W2} / \delta \log P$  for RR Lyrae stars as a function of the cluster metallicity. The dashed line shows the relation defined by equation (6).

### 3.2 The metallicity slopes ( $\beta_X$ )

We now follow the procedure employed by Dambis et al. (2013) to estimate the metallicity slopes  $\beta_{W1}$  and  $\beta_{W2}$  of the W1- and W2-band PML relations for RR Lyrae. The following analysis is to a large degree based on our previous paper (Dambis et al. 2013), where we use the metallicity scale of

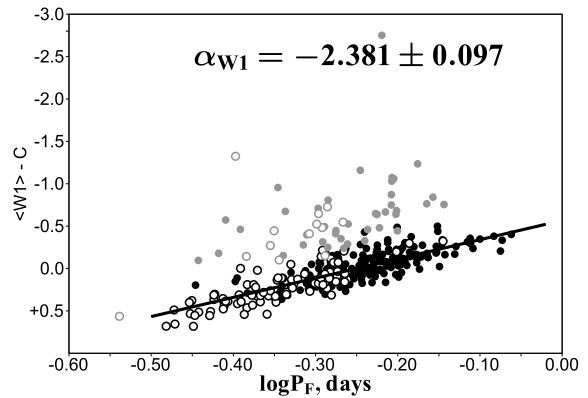


**Figure 8.** The  $PL_{W1}$  relation for the 360 RR Lyrae of our sample. The solid line shows the resulting fit. Filled circles are the RRab variables, open circles are the RRc variables whose periods have been fundamentalised. The gray symbols are the  $3\sigma$ -rejected data points.

Zinn & West (1984), and we therefore use metallicities on this scale throughout this subsection. We make the necessary transformation to the modern scale of Carretta et al. (2009) in the next subsection. We first compute the  $(\langle V \rangle - \langle W1 \rangle)_0$  and  $(\langle V \rangle - \langle W2 \rangle)_0$  intrinsic colour in-

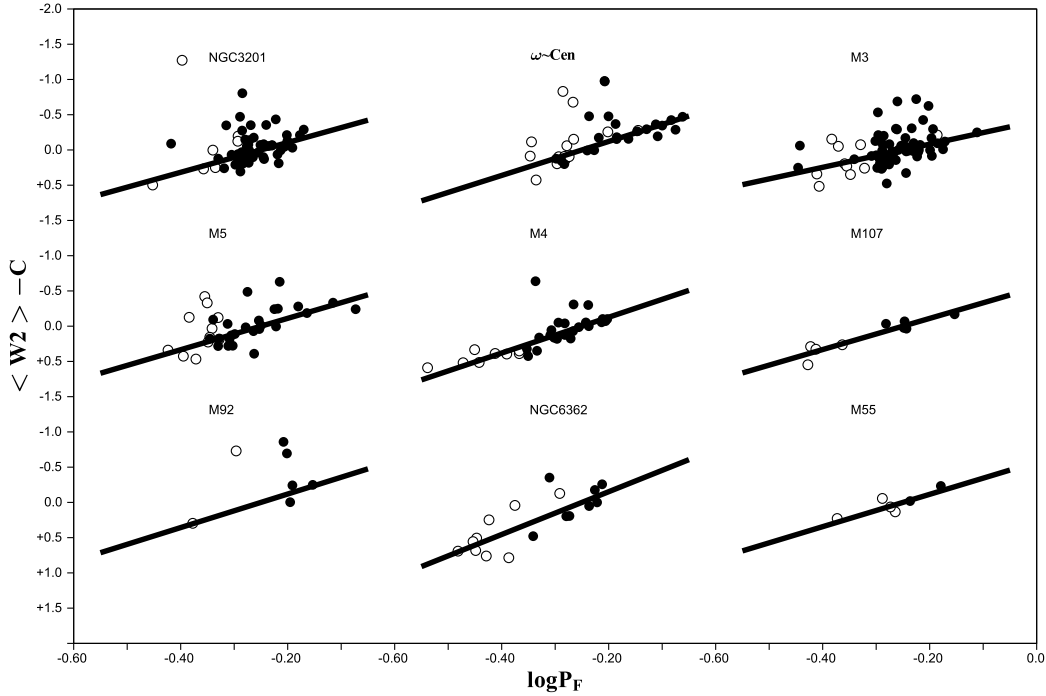


**Figure 5.** The  $PL_{W2}$  relation for the RR Lyrae in 9 calibrator globular clusters. The filled and open circles are the RRab and RRc type variables with fundamentalised periods, respectively. The  $W2$  magnitudes are scaled to the same distance, extinction, and metallicity by subtracting the parameter  $C_{W2}$  for each cluster.

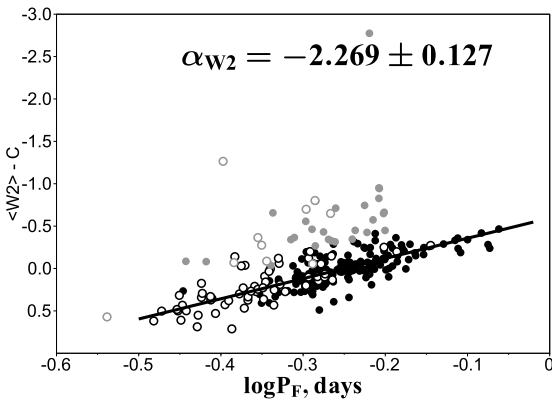


**Figure 9.** The  $PL_{W2}$  relation for the 275 RR Lyrae of our sample. The solid line shows the resulting fit. Filled circles are the RRab variables, open circles are the RRc variables whose periods have been fundamentalised. The gray symbols are the  $3\sigma$ -rejected data points.

indices of 265 field RR Lyrae with  $|b| > 25^\circ$  from Table 2 of Dambis et al. (2013) by dereddening the corresponding observed ( $\langle V \rangle - \langle W1 \rangle$ ) and ( $\langle V \rangle - \langle W2 \rangle$ ) colours using the  $A_V$  values from the above paper (computed using the 3D extinction map by Drimmel et al. (2003)) and the

reddening law by Yuan et al. (2013) ( $R_V = A_V/E_{B-V} = 3.1$ ,  $R_{W1} = A_{W1}/E_{B-V} = 0.18$ , and  $R_{W2} = A_{W2}/E_{B-V} = 0.16$ ). We adopt the  $\langle V \rangle$  and  $\langle W1 \rangle$  intensity-mean magnitudes from the above paper and compute the  $\langle W2 \rangle$  intensity-mean magnitudes from WISE epoch photometry. Like in our previous work, we proceed based on the following established facts. First, the absolute V-band magnitude of RR Lyrae variables depends on metallicity  $[Fe/H]$  and, for a given metallicity, is independent of period. A consensus appears to have emerged concerning the slope of the  $[Fe/H] - \langle M_V \rangle$  relation for RR Lyrae. Thus Baade-Wesselink analyses yield  $\beta_V = 0.20$  (Cacciari et al. 1992),  $\beta_V = 0.21 \pm 0.05$  (Skillen et al 1993), and  $\beta_V = 0.20 \pm 0.04$  (Fernley et al. 1998b), whereas Gratton et al. (2004) and Federici et al. (2012) estimate the slope to be  $\beta_V = 0.214 \pm 0.047$  and  $\beta_V = 0.25 \pm 0.02$ , respectively, based on observations of RR Lyrae in the LMC and horizontal-branch stars in M31 globular clusters, respectively. Like in our previous study, we try to remain as “empiric” as possible and therefore we adopt the simple (unweighted) average of the latter two estimates

$$\langle M_V \rangle = \gamma_V + 0.232(\pm 0.020) \cdot [Fe/H]_{ZW}, \quad (7)$$

because they are based on the sole geometric assumption that the stars involved in both cases are practically at the same distance from us. Second, given the  $\alpha_{W1} = -2.381 \pm 0.097$  and  $\alpha_{W2} = -2.269 \pm 0.127$  slopes derived above, the  $W1$ - and  $W2$ -band PML relations for RR Lyrae have the form:



$$\langle M_{W1} \rangle = \gamma_{W1} + \beta_{W1} \cdot [Fe/H]_{ZW} - 2.381 \cdot \log P_F \quad (8)$$

and

$$\langle M_{W2} \rangle = \gamma_{W2} + \beta_{W2} \cdot [Fe/H]_{ZW} - 2.269 \cdot \log P_F, \quad (9)$$

respectively. We then subtract equations (8) and (9) from equation (7) to obtain:

$$\begin{aligned} (\langle V \rangle - \langle W1 \rangle)_0 &= \langle M_V \rangle - \langle M_{W1} \rangle = \\ &= (\gamma_V - \gamma_{W1}) + (0.232 - \beta_{W1}) \cdot [Fe/H]_{ZW} + 2.381 \cdot \log P_F \end{aligned} \quad (10)$$

and

$$\begin{aligned} (\langle V \rangle - \langle W2 \rangle)_0 &= \langle M_V \rangle - \langle M_{W2} \rangle = \\ &= (\gamma_V - \gamma_{W2}) + (0.232 - \beta_{W2}) \cdot [Fe/H]_{ZW} + 2.269 \cdot \log P_F, \end{aligned} \quad (11)$$

respectively. We finally subtract the terms  $2.381 \cdot \log P_F$  and  $2.269 \cdot \log P_F$  from both sides of equations (10) and (11) to obtain:

$$\begin{aligned} (\langle V \rangle - \langle W1 \rangle)_0 - 2.381 \cdot \log P_F &= \\ &= (\gamma_V - \gamma_{W1}) + (0.232 - \beta_{W1}) \cdot [Fe/H]_{ZW} \end{aligned} \quad (12)$$

and

$$\begin{aligned} (\langle V \rangle - \langle W2 \rangle)_0 - 2.269 \cdot \log P_F &= \\ &= (\gamma_V - \gamma_{W2}) + (0.232 - \beta_{W2}) \cdot [Fe/H]_{ZW} \end{aligned} \quad (13)$$

Our calibrating stars now are 265 field RR Lyraes from Table 2 from Dambis et al. (2013) located at Galactic latitudes  $|b| \geq +25^\circ$  and with known  $V$ -,  $W1$ -, and  $W2$ -band intensity mean magnitudes. We finally solve equations (12) and (13) for parameters  $(\gamma_V - \gamma_{W1})$ ,  $(0.232 - \beta_{W1})$  and  $(\gamma_V - \gamma_{W2})$ ,  $(0.232 - \beta_{W2})$ , respectively, to find:

$$\begin{aligned} (\langle V \rangle - \langle W1 \rangle)_0 &= \\ &= 1.908(\pm 0.019) + 0.126(\pm 0.012) \cdot [Fe/H]_{ZW} + 2.381 \cdot \log P_F \end{aligned} \quad (14)$$

with a scatter of 0.087, and

$$\begin{aligned} (\langle V \rangle - \langle W2 \rangle)_0 &= \\ &= 1.853(\pm 0.018) + 0.113(\pm 0.012) \cdot [Fe/H]_{ZW} + 2.269 \cdot \log P_F \end{aligned} \quad (15)$$

with a scatter of 0.083, implying  $\beta_{W1} = 0.106 \pm 0.023$  and  $\beta_{W2} = 0.119 \pm 0.023$ , respectively.

### 3.3 The zero points ( $\gamma_X$ )

Given our recent statistical-parallax calibration of the  $[Fe/H] - \langle M_V \rangle$  relation (Dambis et al. 2013):

$$\langle M_V \rangle = +1.094(\pm 0.091) + 0.232(\pm 0.020) \cdot [Fe/H]_{ZW}, \quad (16)$$

we immediately obtain the following RR Lyrae PML relations in the  $W1$  and  $W2$  bands:

$$\begin{aligned} \langle M_{W1} \rangle &= -0.814(\pm 0.093) \\ &- 2.381(\pm 0.097) \cdot \log P_F + 0.106(\pm 0.023) \cdot [Fe/H]_{ZW} \end{aligned} \quad (17)$$

and

$$\begin{aligned} \langle M_{W2} \rangle &= -0.759(\pm 0.093) \\ &- 2.269(\pm 0.127) \cdot \log P_F + 0.119(\pm 0.023) \cdot [Fe/H]_{ZW}. \end{aligned} \quad (18)$$

A transformation to the modern metallicity scale via equation

$$[Fe/H]_{Carretta} = 1.105[Fe/H]_{ZW} + 0.160 \quad (19)$$

(Carretta et al. 2009) yields:

$$\begin{aligned} \langle M_{W1} \rangle &= -0.829(\pm 0.093) \\ &- 2.381(\pm 0.097) \cdot \log P_F + 0.096(\pm 0.021) \cdot [Fe/H]_{Carretta} \end{aligned} \quad (20)$$

and

$$\begin{aligned} \langle M_{W2} \rangle &= -0.776(\pm 0.093) \\ &- 2.269(\pm 0.127) \cdot \log P_F + 0.108(\pm 0.021) \cdot [Fe/H]_{Carretta}. \end{aligned} \quad (21)$$

We perform another calibration of the zero points  $\gamma_{W1}$  and  $\gamma_{W2}$  based on intensity-mean  $W1$ - and  $W2$ -band magnitudes and HST FSG trigonometric parallaxes of four RR Lyraes adopted from Madore et al. (2013) and Benedict et al. (2011), respectively,  $\gamma_{W1,HST} = -1.135 \pm 0.077$  and  $\gamma_{W2,HST} = -1.088 \pm 0.077$  for the metallicity scale of Zinn & West (1984) and  $\gamma_{W1,HST} = -1.150 \pm 0.077$  and  $\gamma_{W2,HST} = -1.105 \pm 0.077$  for the metallicity scale of Carretta et al. (2009). Hence the HST trigonometric-parallax based calibrations are:

$$\begin{aligned} \langle M_{W1,HST} \rangle &= -1.135(\pm 0.077) \\ &- 2.381(\pm 0.097) \cdot \log P_F + 0.106(\pm 0.023) \cdot [Fe/H]_{ZW} \end{aligned} \quad (22)$$

and

$$\begin{aligned} \langle M_{W2,HST} \rangle &= -1.088(\pm 0.077) \\ &- 2.269(\pm 0.127) \cdot \log P_F + 0.117(\pm 0.023) \cdot [Fe/H]_{ZW}. \end{aligned} \quad (23)$$

Or, for the metallicity scale of Carretta et al. (2009):

$$\begin{aligned} \langle M_{W1,HST} \rangle &= -1.150(\pm 0.077) \\ &- 2.381(\pm 0.097) \cdot \log P_F + 0.096(\pm 0.021) \cdot [Fe/H]_{Carretta} \end{aligned} \quad (24)$$

and

$$\begin{aligned} \langle M_{W2,HST} \rangle &= -1.105(\pm 0.077) \\ &- 2.269(\pm 0.127) \cdot \log P_F + 0.108(\pm 0.021) \cdot [Fe/H]_{Carretta}. \end{aligned} \quad (25)$$

The HST based distance scales can be seen to be longer than the statistical-parallax based ones by 0.321 and 0.329 in terms of distance moduli for the  $PML_{W1}$  and  $PML_{W2}$  relations, respectively. The discrepancy between the HST and statistical-parallax distance scales appears to be important, amounting to  $\sim 2.7 \sigma$  in both cases.

Interestingly, a recent statistical-parallax calibration of the intensity-mean  $V$ -band absolute magnitude ( $\langle M_V \rangle$ ) of RR Lyrae c-type variables by Kollmeier et al. (2012) yields  $\langle M_V \rangle = 0.59 \pm 0.10$  at  $[Fe/H] = -1.59$ , which is  $\sim 0.14$  brighter than our statistical-parallax based estimate (Dambis et al. 2013) and therefore implies the  $\gamma_{W1}$  and  $\gamma_{W2}$  estimates lying almost halfway between those inferred from our statistical-parallax solution and from HST FSG trigonometric parallaxes. The corresponding  $\gamma_{W1}$  and  $\gamma_{W2}$  zero points prove to be  $\sim \sigma$  brighter than those implied by our calibration and  $\sim 1.4\sigma$  fainter than those implied by HST parallaxes and, perhaps, could reconcile the two. Note, however, that, unlike the study of Kollmeier et al. (2012), which concerns RRc-type variables exclusively distributed mostly in the southern part of the sky and is based on the data for 242 stars, our statistical-parallax analysis involves 387 stars representing a natural mix of RRab and RRc type variables distributed pole-to-pole throughout the entire sky.

**Table 6.** Estimated distances to the calibrator clusters.

Name	$DM_0$ ( $PML_{W1}$ ) statistical parallax zero point	$DM_0$ ( $PML_{W2}$ )	$DM_0$ ( $PML_{W1}$ ) HST trigonometric parallax zero point	$DM_0$ ( $PML_{W2}$ )	$DM_0$ ( $PML_K$ ) (Sollima et al. 2006)
M3	$14.78 \pm 0.02$	$14.74 \pm 0.03$	$15.10 \pm 0.02$	$15.07 \pm 0.02$	15.07
M4	$11.12 \pm 0.02$	$11.11 \pm 0.03$	$11.44 \pm 0.02$	$11.44 \pm 0.03$	11.39
M5	$14.12 \pm 0.02$	$14.17 \pm 0.03$	$14.44 \pm 0.02$	$14.50 \pm 0.03$	14.35
M15	$14.82 \pm 0.03$		$15.14 \pm 0.03$		15.13
M53	$15.98 \pm 0.03$		$16.30 \pm 0.03$		
M55	$13.41 \pm 0.05$	$13.40 \pm 0.06$	$13.73 \pm 0.05$	$13.73 \pm 0.06$	13.62
M92	$14.22 \pm 0.06$	$14.25 \pm 0.07$	$14.55 \pm 0.06$	$14.58 \pm 0.07$	14.65
M107	$13.47 \pm 0.04$	$13.45 \pm 0.05$	$13.79 \pm 0.04$	$13.78 \pm 0.05$	13.76
NGC 3201	$13.13 \pm 0.02$	$13.14 \pm 0.02$	$13.45 \pm 0.02$	$13.47 \pm 0.02$	13.40
NGC 5053	$15.97 \pm 0.04$		$16.29 \pm 0.04$		
NGC 5466	$15.85 \pm 0.04$		$16.17 \pm 0.04$		
NGC 6362	$14.13 \pm 0.03$	$14.18 \pm 0.04$	$14.45 \pm 0.03$	$14.51 \pm 0.04$	14.44
NGC 6723	$14.37 \pm 0.05$		$14.69 \pm 0.05$		
NGC 6934	$15.82 \pm 0.05$		$16.14 \pm 0.05$		
$\omega$ Cen	$13.50 \pm 0.02$	$13.52 \pm 0.03$	$13.82 \pm 0.02$	$13.85 \pm 0.03$	13.72

#### 4 THE DISTANCES TO THE CALIBRATOR CLUSTERS

We estimate the distance moduli of the calibrating clusters using the above PML relations with the zero points based both on the statistical-parallax solution (equations (20) and (21)) and on HST trigonometric parallaxes (equations (24) and (25)). The results are listed in Table 6, where the last column gives the distance moduli estimated by Sollima et al. (2006) based on the  $PML_K$  relation. We find our cluster distance moduli based on the  $PML_{W1}$  and  $PML_{W2}$  relations to be highly consistent with each other with the  $< DM_0(PML_{W1}) - DM_0(PML_{W2}) > = -0.01 \pm 0.03$  and  $< DM_0(PML_{W1}) - DM_0(PML_{W2}) > = -0.02 \pm 0.03$  if computed with the zero points tied to our statistical-parallax solution and HST FSG trigonometric parallaxes, respectively. Furthermore, our cluster distance estimates computed with HST based zero points agree well with those found by Sollima et al. (2006) using their derived the  $PML_K$  relation with the average distance-modulus differences (this paper minus Sollima et al. (2006)) of  $+0.04$  and  $+0.06$  and a scatter of  $0.06$ .

#### 5 CONCLUSIONS

Our analysis of WISE W1- and W2-band epoch photometry for 372 RR Lyrae type variables in 15 Galactic globular clusters combined with V-band and WISE W1- and W2-band photometry of 265 field RR Lyraes at Galactic latitudes  $|b| > 25^\circ$  allowed us to derive the period-metallicity-luminosity relations in the W1 and W2 bands. We derive two sets of appreciably discrepant zero points with one based on our recent statistical-parallax analysis (Dambis et al. 2013) and another one tied to the trigonometric parallaxes of four RR Lyraes measured with the HST FGS (Benedict et al. 2011). The statistical-parallax based calibration yields zero points that are  $0.32^m$  (W1) and  $0.33^m$  (W2) shorter than those calibrated with HST FGS parallaxes. The  $\sim 0.3^m$  difference in the zero points given by two geometric methods is by no means trivial, but this is long-standing issue, which

still remains unresolved. A more detailed discussion can be found in Section 6.1 of our previous paper (Dambis et al. 2013). Let us hope that GAIA will soon resolve the controversy.

We use our calibrations to estimate the distance moduli to 15 calibrator globular clusters of which nine have distance determined using both  $PML_{W1}$  and  $PML_{W2}$  relations. Our distances based on HST zero points agree well with the results of Sollima et al. (2006) with  $+0.04$  and  $+0.06$  distance-modulus differences both for  $PML_{W1}$  and  $PML_{W2}$  and the scatter of  $0.06$  for the W1- and W2-based estimates, respectively.

#### ACKNOWLEDGEMENTS

We thank the anonymous reviewer for the valuable comments, which greatly improved the final version of the paper. This publication makes use of data products from the Wide-field Infrared Survey Explorer, which is a joint project of the University of California, Los Angeles, and the Jet Propulsion Laboratory/California Institute of Technology, funded by the National Aeronautics and Space Administration. This research has made use of NASA's Astrophysics Data System. This work is supported by the Russian Foundation for Basic Research (projects nos. 13-02-00203-a and 11-02-00608-a).

#### REFERENCES

- Benedict G. F., McArthur B. E., Feast M. W., Barnes Th. G., Harrison Th. E., Bean J. L., Menzies J. W., Chaboyer B., Fossati L., Nesvaci N., Smith H. A., Kolenberg K., Laney C. D., Kochukhov O., Nelan E.P., Shulyak D.V., Taylor D., Freedman W.L., 2011, AJ, 142, 187
- Bono G., Caputo F., Castellani V., Marconi M. 1997, A&AS, 121, 327
- Cacciari C., Clementini G., Fernley J. A., 1992, ApJ, 396, 219.

- Castellani M., Caputo F., Castellani V. 2003, *A&A*, 410, 871
- Carretta E., Bragaglia A., Gratton R., D'Orazi V., Lucatello S., 2009, *A&A*, 508, 695
- Catelan, M., Pritzl, B. J., Smith, H. A., 2004, *ApJS*, 154, 633
- Clement C. et al., 2001, *AJ*, 122, 2587
- Cutri R.M. et al. 2012, *VizieR Online Data Catalog*, II/311
- Dambis A. K., Berdnikov L. N., Kniazev A. Y., Kravtsov V. V., Rastorguev A. S., Sefako R., Vozyakova, O. V., 2013, *MNRAS*, 435, 3206
- Drimmel R., Cabrera-Lavers A., Lopez-Corredoira M., 2003, *A&A*, 409, 205
- Feast M.W., Laney C.D., Kinman Th.D., van Leeuwen F., Whitelock P.A., 2008, *MNRAS*, 386, 2115
- Federici L., Cacciari C., Bellazzini M., Fusi Pecci F., Galletti S., Perina S., 2012, *A&A*, 544, 1459
- Fernley J., Skillen I., Carney B. W., Cacciari C., Janes K., 1998, *MNRAS*, 293, L61
- Frolov M. S., Samus N. N., 1998, *Pis'ma Astron. Zh.*, 24, 509
- Gratton R.G., Bragaglia A., Clementini G., Carretta E., Di Fabrizio L., Maio M., Taribello E., 2004. *A&A*, 421, 937
- Harris W. E., 1996, *AJ*, 112, 1487
- Harris W. E., 2010, *arXiv:1012.3224*
- Iben Jr.I. 1974, *ARA&A*, 12, 215
- Klein Ch.R., Richards J.W., Butler N.R., Bloom J.S., 2011, *ApJ*, 738, 185
- Klein Ch.R., Richards J.W., Butler N.R., Bloom J.S., 2011, *Ap&SS*, 341, 83
- Kollmeier J.A., Szczygiel D.M., Burns C.R., Gould A., Thompson I.B., Preston G.W., Sneden C., Crane J.D., Dong S., Madore B.F., Morrell N., Prieto J.L., Shectman S., Simon J.D., Villanueva E., 2013, *ApJ*, 775, 57
- Madore B. F., Hoffman D., Freedman W. L., Kollmeier J.A., Monson A., Persson S. E., Rich J. A., Jr., Scowcroft V., Seibert M. 2013arXiv1308.3160M
- Marconi M., Caputo F., Di Criscienzo M., Castellani M. 2003, *ApJ*, 596, 299
- Poleski R. 2013, 2013arXiv1309.1168P
- Samus N. N., Kazarovets E. V., Pastukhova E. N., Tsvetkova T. M., Durlevich O. V. 2009, *PASP*, 121, 1378
- Sawyer Hogg H., 1973, *Publications of the David Dunlap Observatory, Univ., Toronto*, V. 3, No. 6
- Skillen I., Fernley J. A., Stobie R. S., Jameson R. F., 1993, *MNRAS*, 265, 301
- Sollima A., Cacciari C., Valenti, E. 2006, *MNRAS*, 372, 1672
- van Albada T.S., Baker N. 1973, *ApJ*, 185, 477
- Wright, E. L., Eisenhardt, P. R. M., Mainzer, A. K., et al. 2010, *AJ*, 140, 1868
- Yuan H.B., Liu X.W., Xiang M.S. 2013, *MNRAS*, 430, 2188
- Zinn R., West M. J., 1984, *ApJS*, 55, 45